TRI-PP-84-112
Dec 1984

PIONIC 4F-3D X-RAYS FROM ^{208}PB AND ^{209}BI

A. Olin*, J.W. Forsman, J.A. Macdonald, G.M. Marshall*, T. Numao*, P.R. Poffenberger**, P. van Esbroek
TRIUMF, Vancouver, B. C., Canada

G.A. Beer, D.I. Britton, G.R. Mason
University of Victoria, Victoria, B.C., Canada

A.R. Kunselman
University of Wyoming, Laramie, Wy., U.S.A.

B.H. Olaniyi
University of Ife, Ile-Ife, Nigeria

Abstract

The X-ray energies and widths of the pionic 4f-3d and 5g-4f transitions have been measured in ^{208}Pb and ^{209}Bi. The 3d widths obtained are in reasonable agreement with theory, and do not support the anomalously small values previously reported.

E | Pionic atoms ^{208}Pb, ^{209}Bi; measured 5g-4f and 4f-3d pionic X-rays.

(Submitted to Nuclear Physics A)

*affiliated with University of Victoria, Victoria, B. C., Canada
**affiliated with University of Manitoba, Winnipeg, Man., Canada

1. Introduction

Pionic atoms may be used to study the pion-nucleus strong interaction at low energy. The deviations of the X-ray energies and line widths from their purely electromagnetic values have been measured throughout the periodic table. For a given transition measured in a series of atoms of increasing Z, the absorption widths increase and the intensity of the X-ray is reduced due to pion absorption from the feeding levels, making observation of these X-rays in a large gamma-ray background progressively more difficult. Pionic X-rays are in general well described by an optical model descripton of the pion-nucleus interaction, with agreement between theory and experiment typically at the few percent level. However in a few atoms significantly larger deviations from theory occur for the weakest transitions where the experimental difficulties are most severe. It has proven very difficult to incorporate these results within the optical model framework[1-3]). From a historical perspective, we should view these anomalies with skepticism, since similar cases have in the past not been confirmed when the measurements were repeated with improved experimental techniques.

Until recently, π 4f-3d X-rays had been measured up to Z=60 where the shifts and widths are ~10 KeV [4]). When the 4f-3d X-ray measurements were extended to Ta, Re, Pt, Au, and Bi[5,6]), their measured shifts and widths were a factor 2 to 3 smaller than predicted. These measurements were made possible by use of a Compton suppression spectrometer to reduce the backgrounds. At TRIUMF we have undertaken a measurement of the ^{208}Pb and ^{209}Bi X-rays, exploiting the low-momentum pion beam and a BGO Compton suppressor to obtain somewhat lower backgrounds than were achieved in earlier work. ^{208}Pb was chosen because it is a spherical nucleus, so

there is no hyperfine splitting of the X-ray to deal with, and because the matter distributions of doubly-closed-shell nuclei are particularly easy to calculate. Because of the sensitivity of pionic X-rays to the neutron matter distributions, this knowledge is important in the interpretation of the results. We have repeated the ^{209}Bi measurement for comparison with earlier work, and to further study the background problems in this energy region.

2. Experimental Method

The measurements were performed using the 90 MeV/c π^- beam of the TRIUMF M13 channel. Approximately 4×10^5 stopping pions/sec were registered in a conventional scintillator telescope. The lead target was 40 g of 99% pure ^{208}Pb obtained on loan from Oak Ridge. Both Pb and Bi targets were metallic foils 7 cm diameter and 1 g/cm^2 thick. Two different Ge detectors were used during the data-taking runs, a 15% efficiency p-type and a 10% efficiency n-type detector. Both started with resolutions of ~1.9 keV at 1.3 MeV, which degraded to ~2.2 keV during the runs from radiation damage. The Ge detector was positioned 40 cm from the target in order to allow time-of-flight separation of the neutrons and gammas. The timing achieved was 4 ns FWHM at 1.3 MeV, allowing separation of neutrons up to 30 MeV; this effectively removed the Ge (n,n'γ) backgrounds. The singles count rate above 100 keV in the detector was <3000/sec. The detector was surrounded by a Compton suppression spectrometer which consisted of 16 bismuth germanate (BGO) crystals $80 \times 55 \times 55$ mm^3 mounted in a transverse geometry, as shown in fig. 1. The suppressor was shielded from the target with borated paraffin, lead, copper, and tungsten. Care was taken that the lead shielding could not be viewed directly by the Ge counter. Details on the performance of the

spectrometer have been published separately[7]). The Ge detector ADC was dynamically stabilized in zero and slope using two calibration peaks in the spectrum, and the energy and time relative to the pion stop were written to magnetic tape. Calibration source lines from ^{60}Co, ^{137}Cs, ^{198}Au, and positron annihilation were collected simultaneously in random coincidence with stops in the 1 cm thick beryllium degrader. During the early part of each run, the BGO veto was used to set a bit in a pattern register, and the energy, time, and BGO crystal segment of the vetoing pulse were recorded. This information was used to study the in-beam behavior of the Compton suppression system. The bulk of the data were accumulated with the BGO veto included in the event trigger, which reduced by a factor of four the number of magnetic tapes required. In order to reduce pileup distortion in the photon spectrum, all photons separated in time by less than 35 μs were rejected.

3. Data Analysis

3.1 ^{208}Pb data

The ^{208}Pb data were accumulated over two running periods and analysed in three different data sets. This was made necessary because different Ge detectors were used in set 1 and sets 2 and 3, and because the Ge lineshape changed between sets 2 and 3 due to radiation damage to the detector. Fig. 2 shows the data from set 3 in the region of the π 4-3 X-ray, consisting of approximately 35% of the total data. The fitting function consisted of a broad Lorenzian line for the π 4-3 X-ray folded with the gamma-ray resolution function, narrower folded Lorenzians for the π 8-4 and π 9-4 X-rays whose widths were obtained from the π 5-4 X-ray, a number of gamma-rays from pion absorption and an exponentially varying background. The gamma-ray lineshape, modelled by a Gaussian peak with a

two-parameter exponential tail and including a background step at the peak position, was obtained by fitting the calibration lines accumulated simultaneously with the data. The effect of the variation of the detector efficiency over the broadened lines was also taken into account. A chi-squared minimization code, which allowed one to omit selected areas within the fitting window, was used, so that the sensitivity of the fit to possible contaminants could be explored.

The results are shown in Table 1. Since the scatter among the three Pb data sets is consistent with the statistical uncertainties, the weighted mean is used for the final result. The quality of the data has permitted a more thorough evaluation of the systematic uncertainties than was possible in earlier work. From the fact that the background in the prompt time spectrum is reduced 50% less than that of the in-beam source spectrum, we conclude that it has a significant photopeak component consisting of continuum and weak discrete gamma-rays from the pion absorption process. Two models for the background shape, linear and exponentially decreasing, were used in the fitting, and the effect of omitting areas of the fitting region, or of allowing additional weak contaminant peaks on top of the 4-3 X-ray was explored. Most of the gammas in this region have been identified with levels of Tl isotopes and the weakest lines included in the fit have a yield of $<10^{-3}$ per pion stop. The fit has been performed over three fitting regions: 1144-1397 keV, 1110-1397 keV, and 1074-1488 keV. Reasonably consistent results were obtained for these regions except for the linear background 1074-1488 keV region combination, where the chi-square was increased and the X-ray line width reduced compared to the linear fit over smaller regions. For this reason the exponential background shape was adopted for the final result.

The difference between these two fits was used to estimate the uncertainty due to the background shape to be ±0.1 keV in energy and ±2.8 keV in width. Uncertainties in the detector response function contributed ±0.6 keV and ±1.1 keV, and the contribution from contamination peaks was estimated to be ±0.8 keV and ±3.5 keV. Since these contributions are independent, they have been combined in quadrature to obtain a total systematic error of ±1.0 keV in the energy and ±4.6 keV in the width. The chi-square obtained in our best fit was 1.03 per degree of freedom, showing that our model gives a consistent overall description of the spectrum region. The peak-to-background amplitude obtained for ^{208}Pb spectrum region was 1:2, compared to 1:2 obtained by the NIKHEF group for the more intense π Au X-ray[6]) and to 1:7 for their π Bi data[5]). However, we have chosen to treat systematic effects in a rather conservative manner, so that the quoted errors for our Pb and their Bi X-rays are nearly the same.

The Pb π 5-4 X-ray has been measured with sufficient statistics that the strong interaction shift and width is fitted with accuracy limited by knowledge of the detector response function. The quality of the fit is shown in fig. 3. This X-ray has not been previously measured using a ^{208}Pb separated isotope target. The ratio of the intensities of the π 4-3 and π 5-4 X-rays is determined by the 4f strong interaction width, which gives the pion absorption width of this state. The measured intensity ratio is 9.6%±1.9% after corrections for the detector efficiency and self-absorption in the target. The uncertainty in this ratio includes the systematic width uncertainty on the π 4-3 peak area and the uncertainty in the relative detector efficiency due to the tight timing cuts used and the variation of timing with energy. From the measured 5-4

X-ray width and a calculation of the pionic atom cascade using an initial population of the n=15 substates that reproduces the intensities of the ng-4f X-ray series we would expect 12%±1%. However the width of 80 keV predicted by the optical model is also consistent with this intensity ratio.

3.2 ^{209}Bi data

The fit in the region of the ^{209}Bi 4-3 X-ray is shown in fig. 4. In this case the number of contaminant gammas from pion absorption is much higher, and the background is consequently less well-determined. The peak-to-background ratio is only 1:3.5. Again the systematic errors are dominant, especially the possible structure in the background.

However, even when the systematic effects are adjusted to their most favorable values it is not possible to get a reasonable fit to our data using the energy and width of ref. [5]). Differences in the analysis are a much larger fit region used in the present work (1155-1425 keV compared with 1280-1330 keV) and the inclusion of additional γ-rays and of the 9-4 and 10-4 pionic X-rays, which were too weak to be distinguished in the earlier work.

The ^{209}Bi 5-4 X-ray is well fitted (fig 5), and the ratio of intensities is 9.4%±2%, again consistent with the measured 4f width. The width of the 5-4 X-ray is consistent with the result obtained by Batty et al.[8]), and somewhat wider than seen by Beetz et al.[9]). We have not included hyperfine effects in the analysis of the ^{209}Bi transitions. These splittings have been calculated by Konijn et al.[5]) to be 2.1 keV for the π 4-3 and 400 eV for the π 5-4 transitions.

4. Results

The existence of a series of broad structures with approximately the expected energies and intensities in Ta, Re, Pt, Au, Pb, and Bi confirms

their identification as pionic 4-3 X-rays. There remains the question of whether reduced strong interaction effects are reflected in the present results. In order to display the trends in the strong interaction effects, we have calculated shifts and widths of the atomic levels from the measured transition values by correcting for the calculated shift of the 5g level and the strong interaction and radiative widths of the 5g, 4f, and 3d levels. The electromagnetic level energies were computed including the nuclear finite size, higher order vacuum polarization, Lamb shift, electron screening, and reduced mass corrections. Fermi distributions were used for the nuclear charge distributions with parameters c=6.624 fm, t=2.3 fm for Pb and c=6.689 fm, t=2.3 fm for Bi taken from muonic X-ray measurements[10]).

In fig. 6 these results are compared to optical model calculations including the dependence on the difference of the neutron matter and proton matter distribution rms radii Δ. The value of Δ (^{208}Pb) has been measured in proton scattering at 1 GeV to be 0.14±.04 fm[11]), while Hartree Fock calculations by Angeli et al.[12]) give 0.20 fm. A calculation using the method of Negele and Vautherin[13]) also gives Δ(^{208}Pb)=0.205 fm and Δ(^{209}Bi)=0.199 fm[14]). The optical parameters used are "set (b)" from ref. [8] and "set (i)" from ref. [16]; they differ in their treatment of the absorption terms. Also included are some values calculated by Seki[3]) using a model which includes angular transformation and Coulomb gauge terms. We believe, based on the results of Batty et al.[2]) and Seki[3]) that these models fairly reflect the range of theoretical predictions. Considering the variations among the calculations, both shifts and widths are reasonably consistent with the theory. The strong interaction quadrupole splitting of the Bi 4f level is

significant and accounts for the large width compared to Pb. The worst agreement is with ^{208}Pb Γ_{3d}, which is low by about two standard deviations. However, since such discrepancies also occur for some lower Z atoms, we would not wish to overemphasize the significance of this result.

Tauscher et al.[17]) have recently calculated the p-wave absorption process within the framework of the isobar-hole model. Saturation effects are predicted because a strongly nonlinear density dependence is obtained. In heavy nuclei the effect is to decrease Γ_{3d} by 10-20%, while Γ_{4f} is increased by a similar amount. Our results appear to support this prediction.

References

[1]C.J. Batty, E. Friedman, and A. Gal, Nucl. Phys. **A402** (1983) 411.

[2]R. Seki, Marmal Aid Preprint MAP-46 (1983).

[3]J.G.J. Olivier, M. Theis, and J. Koch; Nucl. Phys. A429 (1984) 477.

[4]A.R. Kunselman, P. Robertson, R.J. Powers, F. Boehm, J.P. Miller, A. Zehnder, and J. Jarmer, Phys. Rev. **15C** (1977) 1801.

[5]J. Konijn, J.K. Panman, J.H. Koch, W. van Doesburg, G.T. Ewan, T. Johansson, G. Tibell, K. Fransson and L. Tauscher, Nucl. Phys. **A326** (1979) 401.

[6]J.F.M. d'Achard van Enschut, J.B.R. Berkhout, W. Duinker, C.W.E. van Eijk, W.H.A. Hesselink, T. Johansson, T.J. Ketel, J.H. Koch, J. Konijn, C.T.A.M. det Laat, W. Lourens, G. van Middelkoop and W. Poeser, Phys. Lett. **36B** (1984) 24.

[7]A. Olin, P.R. Poffenberger, and D.I. Britton, Nucl. Instr. and Methods **222** (1984) 463.

[8]C.J. Batty, S.F. Biagi, E. Friedman, S.D. Hoath, J.D. Davies, G.J. Pyle, G.T.A. Squier, D.M. Asbury, and A. Guberman, Nucl. Phys. **A322** (1979) 445.

[9]R. Beetz, F.W.N. De Boer, K. Fransson, J. Konijn, J.K. Panman, L. Tauscher, and G. Tibell, Nucl. Phys. **A300** (1978) 369.

[10]R. Engfer, H. Schneuwly, J.L. Vuillemier, H.K. Walter, and A. Zehnder, Atom Data and Nucl. Data Tables **14** (1974) 409.

[11]G.W. Hoffman, L. Ray, M. Barlett, J. McGill, G.S. Adams, G.J. Igo, F. Irom, A.T.M. Wang, C.A. Witten, R.L. Boudrie, J.F. Amann, C. Glashausser, N.M. Hintz, G.S. Kyle and G.S. Blanpied, Phys. Rev. **C21** (1980) 1488.

[12]I. Angeli, M. Beiner, R.J. Lombard and J. Mass, J. Phys. G: Nucl. Phys. **6** (1980) 303.

[13]J.W. Negele and D. Vautherin, Phys. Rev. C 5 (1972) 1472.

[14]Y. Tanaka, Private communication.

[15]H. Schmitt, L. Tauscher, G. Backenstoss, S. Charlambus, H. Daniel, H. Koch, and G. Poelz, Phys. Lett. **27B** (1968) 530.

[16]A.R. Kunselman, R.J. Powers, M.V. Hoehn, and E.B. Shera, Nucl. Phys. **405** (1983) 627.

[17]L. Tauscher, C. Garcia-Recio, and E. Oset, Nucl. Phys. A **415** (1984) 333.

Table 1. Measured Transition Energies and Widths

Transition	Energy keV	Error stat	Error sys	EM keV	Shift keV	Width keV	Error stat	Error sys	Area	Ref
Pb 4-3	1274.7	±.6	±1.0	1251.0	23.7	47.4	±2.6	±4.6	16200	present
Pb 5-4	575.44	±.02	±.05	573.68	1.76	1.30	±.03	±.08	270000	present
Pb 5-4 nat	575.357	±.017		573.697	1.66	1.299	±.045			a
Pb 5-4 nat	575.56	±.25			1.76	1.1	±.3			b
Bi 4-3	1312.0	±1.8	±3.0	1282.40	30.4	71.2	±8.4	±21*	15000	present
Bi 4-3	1301.3	±1.3	±.6		19.7	25.4	±5.3	±2.7	3000	c
Bi 5-4	589.90	±.05	±.04	588.13	1.77	1.49	±.02	±.04*	284000	present
Bi 5-4	589.68	±.10		587.85	1.59	1.33	±.07			d
Bi 5-4	589.840	±.060		588.021	1.82	1.37	±.14			a

* includes hyperfine broadening
a)Reference 8 b) Reference 15 c) Reference 5 d) Reference 9

Figure Captions

1. Arrangement of the experimental apparatus.
2. Fits to the ^{208}Pb π 4-3 xrays. For clarity the data has been rebinned to 2.8 keV/bin, but the fits were done with 0.57 keV/bin. The different fit models shown, characterized by the x-ray energy E and width Γ, were used in the evaluation of the systematic uncertainties. Gaps in the fit lines denote regions omitted from the fit.
3. Fit to the ^{208}Pb π 5-4 xray.
4. Fits to the ^{209}Bi π 4-3 x-ray. The presentation is similar to fig. 1. Also included is a fit with the x-ray position and width fixed at its previously reported value of E=1301 keV, Γ=25 keV.
5. Fit to the ^{209}Bi π 5-4 x-ray. The fit model does not include strong hyperfine effects.
6. Level shifts and widths are shown as a function of $\Delta=\langle r^2\rangle^{1/2}-\langle r^2\rangle^{1/2}$. The calculations are from Kunselman et al. [▲, ref. 16)], Batty et al. [● , ref. 8)] and Seki [■, ref. 3)]. The cross-hatched band shows the experimental value with its 1σ error.

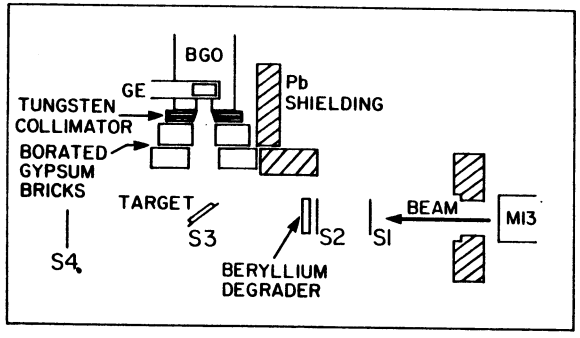

Fig. 1

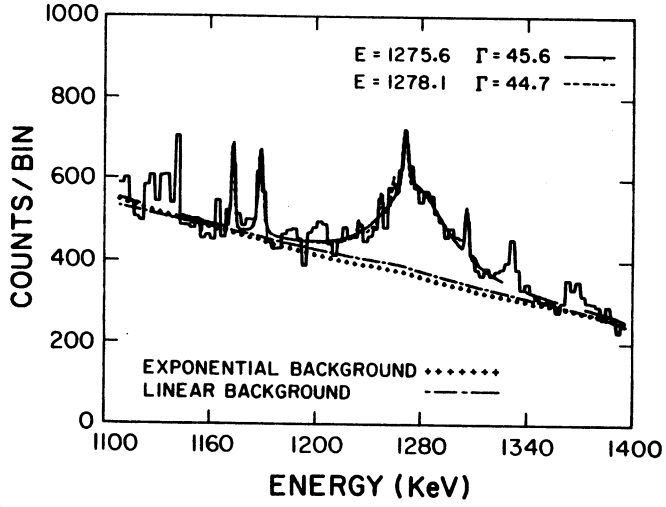

Fig. 2

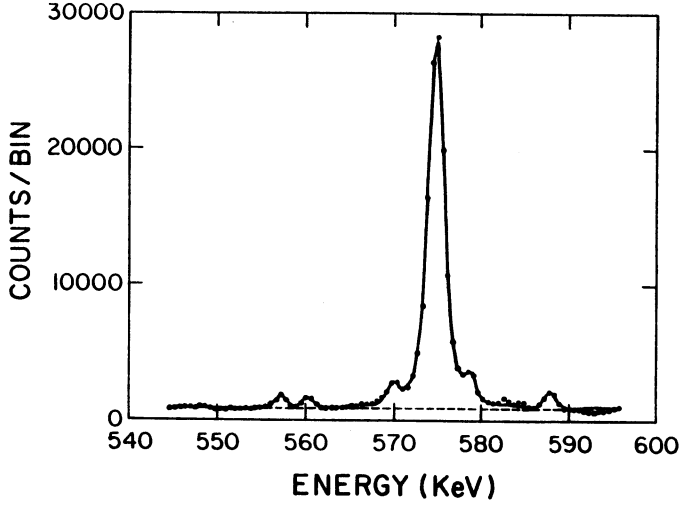

Fig. 3

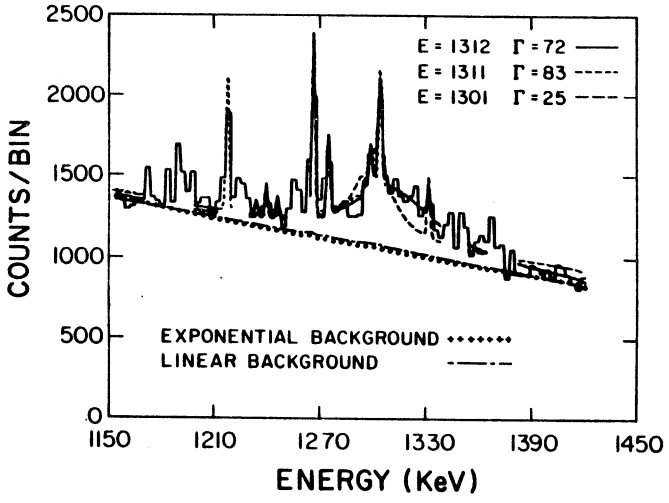

Fig. 4

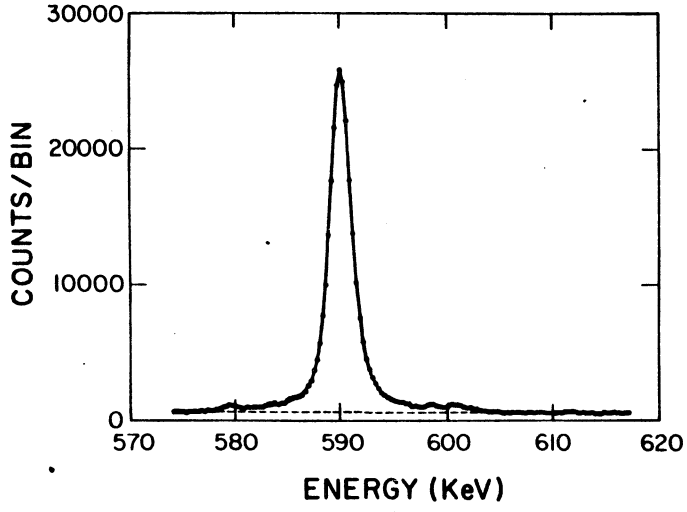

Fig. 5

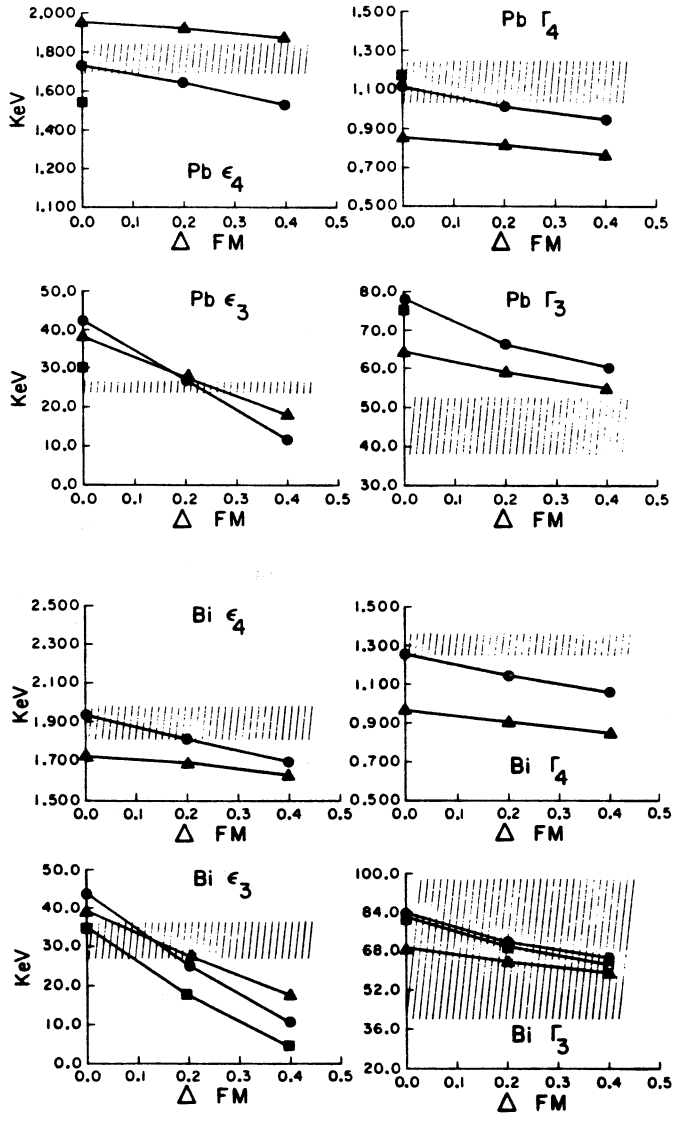

Fig. 6